

**PROPERTIES OF PORTLAND CEMENT MAJOR CONSTITUENTS
USING MOLECULAR DYNAMIC SIMULATIONS¹**

W. Wu^a, Ahmed Al-Ostaz^{b,*}, A. H.-D. Cheng^c, C. R. Song^d

^a Research Associate, Department of Civil Engineering, University of Mississippi,
University, MS 38677, USA

^{b*} Associate Professor, Department of Civil Engineering, University of
Mississippi, University, MS 38677, USA

^c Professor, Department of Civil Engineering, University of Mississippi,
University, MS 38677, USA

^d Assistant Professor, Department of Civil Engineering, University of Mississippi,
University, MS 38677, USA

*Corresponding author. Tel.: +1662 915 5364; fax: +1662 915 5523.
E-mail address: alostaz@olemiss.edu (A. Al-Ostaz).

¹ Manuscript submitted to Journal of Cement and Concrete Research. October 2008.

Abstract:

Commercially available Molecular Dynamics (MD) software Materials Studio utilizing Discover and Forcite molecular dynamics tools is used to compute the elastic constants of major Portland Cement (PC) compounds (e.g. C₃S and alite, C₂S and belite, and C₃A). The elastic constants of C₃S, C₂S and C₃A reported in this paper were calculated using COMPASS, Universal and DREIDING Forcefields. The combination of different simulation cell sizes, simulation tools and force fields is evaluated. Simulation of C₃S and C₂S using Forcite with COMPASS forcefield results in elastic constants that match nanoindentation experimental values reported in the literature. On the other hand, using Forcite with DREIDING forcefield yields a good estimation of C₃A mechanical properties.

1. INTRODUCTION

Portland cement concrete is presently the most widely used construction material. The consumption of concrete in the world measures more than two tons per year for each person on earth [1]. Concrete has emerged as the most widely used engineering material because:

- it possesses excellent resistance to water;

The cement chemistry abbreviation used in this paper:
(C₃S = 3.CaO.SiO₂, C₂S = 2.CaO.SiO₂, C₃A = 3.CaO.Al₂O₃, C₄AF = 4.CaO.Al₂O₃.Fe₂O₃).

- structural concrete elements can be easily formed into a variety of shapes and sizes;
- concrete is usually the cheapest and most readily available material on the job site;
- the production of concrete requires considerably less energy input compared to most other engineering materials; and
- a large amount of many industrial wastes can be recycled as substitute for various virgin material components in concrete.

To produce high quality, long-lasting concrete structures, cements of a high and consistent quality must be employed. Worldwide, the cement industry spends countless hours assuring the quality of its products, mainly based on laboratory tests. In the U.S., most physical testing of cements is performed according to ASTM standards [2-3]. However, very limited literature is available on evaluating the mechanical properties of PC constituents. Those constituents are usually in the nanoscale range. A critical issue for predicting mechanical properties of such materials is the ability to understand, model, and simulate the behavior of cement compounds and to make the connection between the nanostructure properties and their macroscopic functions.

Cement is made primarily from limestone, which is crushed to a powder form and heated to a very high temperature (1500°C) in a kiln; during the process the limestone undergoes a transformation, storing energy in the cement powder. This is why cement production accounts for an estimated 5 to 10 percent of the world's CO₂ emission, one of the primary greenhouse contributors to global warming.

Thus, if we can reduce CO₂ emissions from the world's cement manufacturing by 10 percent, we would have accomplished one-fifth of the Kyoto Protocol's goal of a 5.2 percent reduction in CO₂ emissions from industrialized nations. Realizing how the cement and concrete industries influence the already fragile environment, researchers are striving to make "greener concrete". In order to understand the fundamental behavior of PC materials, performing atomic simulations is recommended in order to take the work a step deeper into the structure of this ubiquitous material cement [4-5].

Limited work is available in the literature on obtaining the mechanical properties of PC constituents (phases) experimentally. Velez, et al. [6] used nanoindentation and resonance frequency techniques to measure the elastic modulus and hardness of PC clinker constituents. Using the nanoindentation technique, they found that, at the microscopic scale, the elastic Young's moduli of PC phases range between 125GPa for C₄AF to 145GPa for C₃A. Whereas, using the resonance frequency technique they found that the elastic moduli, at the macroscopic scale, fall into the range of 147GPa and 160GPa [5]. They also concluded that the elastic moduli of the C₃S, C₂S, C₃A phases decrease by about 35% when the porosity decreases by 15%. Boumiz, et al [7] showed that the elastic modulus of unhydrated cement is about 117.6GPa using nanoindentation tests. Granju [8] measured the elastic moduli of clinker on polished blocks. By extrapolating at zero porosity, he found an elastic modulus for the clinker ranging between 60 and 300 GPa. The scatter of the results was due to the cracks introduced during the preparation of the sample. Other techniques such as statistical model and soft computing techniques, gene

expression programming (GEP), and neural networks (NNs) are also promising tools for the prediction of cement strength [9-10].

The Molecular Dynamics (MD) method has been widely used in simulating the behavior of materials such as carbon nanotube (CNT) and CNT reinforced nanocomposites by number of researchers [11-14]. To date, there is no existing literature on using molecular dynamics to evaluate the mechanical properties of unhydrated PC. In this paper, we used a molecular dynamics (MD) simulation approach to obtain the mechanical properties of single crystal and polycrystals of major phases of PC (C_3S and alite, C_2S and belite, C_3A). These three phases account for more than 90% of the total mass of cement clinkers [15]. The crystallographic data of the three single crystals used in this research is given in Table 1 and the corresponding unit cell crystal structures are shown in Figures 1-3. We used commercially available molecular dynamics software Materials Studio[®]. Three different forcefields were used: Condensed-phase Optimized Molecular Potentials for Atomic Simulation Studies (COMPASS) [16], Universal forcefield (UFF) [17] and DREIDING forcefield [18]. COMPASS is incorporated in both Discover and Forcite molecular dynamics modules, while Universal and DREIDING are only available in the Forcite molecular dynamics module. Moreover, we consider the different sizes of the supercell in order to better represent the properties of the crystals [19].

2. CRYSTAL STRUCTURES OF THE CONSTITUENTS OF CEMENT

ASTM C150 defines Portland cement as hydraulic cement produced by pulverizing clinkers consisting essentially of hydraulic calcium silicates, and usually containing one or more forms of calcium sulfate and interground addition. Clinkers are 5-25 mm-diameter nodules of a sintered material which is produced when a raw mixture of predetermined composition is heated to a high temperature. Cement has four main clinker minerals: alite (C_3S), belite (C_2S), aluminate C_3A , and brownmillerite (C_4AF). Calcium silicates are the primary constituents of PC. During the manufacturing process, C_3S is formed at a temperature above 1250°C through a reaction of C_2S and C. It undergoes several polymorphic phase transformations at different temperatures. C_2S also has several polymorphs: α - C_2S , β - C_2S and γ - C_2S . C_3S is the most important compound because it accounts for the binding properties of cement and accounts for 55-65% of the total mass of cement. The crystal structure of C_3S [20] is built up from SiO_4^{4-} tetrahedral structure with Ca^{2+} in the corners and oxygen in the center as shown in Table 1 and Figure 1. Dicalcium silicate or C_2S is another important constituent of Portland cement. The structure is built up of isolated SiO_4 tetrahedral and Ca ions which looks like strings of alternating Ca ions and tetrahedral since four of the eight Ca ions are positioned alternately above and below SiO_4 tetrahedral in the y direction [21] as shown in Table 1 and Figure 2. Compared with C_3S and C_2S , C_3A does not exhibit polymorphism. It is a cubic structure built from Ca^{2+} ions and highly puckered rings of six AlO_4 tetrahedral [22] as shown in Table 1 and Figure 3.

3. METHODS

We used the Molecular Dynamics simulation method to study the mechanical properties, namely modulus of elasticity, Poisson's Ratio, bulk and shear modulus. Molecular Dynamics is one of the modeling schemes of molecular mechanics (the others are: energy minimization, conformational analysis and stochastic methods or Monte Carlo methods) [23], which directly calculates the potential energy surface by solving the classic Newton's equation of motion:

$$-\frac{dE}{dR} = m \frac{d^2 R}{dt^2} \quad (1)$$

where E is potential energy, R represents position of the nuclei, m is mass and t is time. Commercially available Molecular Dynamics (MD) software Materials Studio [24] was utilized in the simulation.

MD Simulation Conditions

1a×1b×1c, 2a×2b×2c (a,b,c: unit cell dimensions; corresponding to 1,8 unit cells) supercells were used in our simulations (3a×3b×3c supercell is, also, used in simulating C₂S). The number of atoms in the simulation systems ranges from 28 for one unit cell of C₂S to 2112 atoms for the 2a×2b×2c C₃A supercell. Molecular Dynamics simulation starts from energy minimization which aims to optimize a structure with a high energy configuration. We used the “smart minimization method” which automatically combines the steepest descent, conjugate gradient and Newton method. Starting with the steepest descent method, followed by the

conjugate gradient method and ending with a Newton method, steepest descent can quickly reduce the energy during the initial interactions and it should be used when the gradients of the energy configuration are far from the minimum. The Newton method is usually for small systems and it is very efficient near the energy minimum, while the conjugate gradients method is appropriate for larger systems. Next, we used the NPT (constant number of atoms, N , constant pressure, P , and constant temperature, T) canonical ensemble since it allows both the unit cell size and shape to change. The temperature is set to $T=25^{\circ}C$ ($298^{\circ}K$) and the pressure is at $P=0.1$ MPa. The Anderson thermostat temperature control method and Parrinello pressure control method were used with Discover molecular dynamics tool while the Nosé thermostat temperature control method and the Berendsen pressure control method were used with a Forcite molecular dynamics tool (Parrinello is not available for Forcite). We chose the time step as 1 femtosecond (fs, 10^{-15} sec) since 1fs is suitable for most purposes [25]. The dynamics time ranges from 100 to 400 picoseconds (ps, 10^{-12} sec) depending on the size of the simulating system, which ensures thermodynamic equilibrium and the convergence of energy with a reasonable computation time. The summation methods for van der Waals and Coulomb forces were all atom-based (Cutoff distance, spline width and buffer width were 12.5Å, 3.0 and 1.0 Å).

Forcefields

The solution of Newton's equation (see Eq. 1) in MD needs an empirical fit to the potential energy surface, which is often called a forcefield. The forcefield describes approximately the potential energy hypersurface on which the atomic

nuclei move around. The proper choice of a forcefield is a crucial step in MD simulation [25]. The three most commonly used forcefields have been applied to this study: COMPASS, UFF and DREIDING forcefields. In order to better understand and compare the three forcefields, we list their functional forms of potential energy here.

COMPASS forcefield is a high quality general *ab initio* forcefield, which has been widely used in simulations of liquids, crystals, and polymers. The functional form of the COMPASS forcefield [25] is:

$$\begin{aligned}
E_{total}^{compass} &= E_{valence} + E_{crossterm} + E_{non-bond} \\
&= \sum_b \left[K_2 (b - b_0)^2 + K_3 (b - b_0)^3 + K_4 (b - b_0)^4 \right] \\
&+ \sum_\theta \left[H_2 (\theta - \theta_0)^2 + H_3 (\theta - \theta_0)^3 + H_4 (\theta - \theta_0)^4 \right] \\
&+ \sum_\phi \left[V_1 [1 - \cos(\phi - \phi_1^0)] + V_2 [1 - \cos(2\phi - \phi_2^0)] + V_3 [1 - \cos(3\phi - \phi_3^0)] \right] \\
&+ \sum_\chi K_\chi \chi^2 + \sum_b \sum_{b'} F_{bb'} (b - b_0)(b' - b'_0) + \sum_\theta \sum_{\theta'} F_{\theta\theta'} (\theta - \theta_0)(\theta' - \theta'_0) \\
&+ \sum_b \sum_\theta F_{b\theta} (b - b_0)(\theta - \theta_0) + \sum_b \sum_\phi F_{b\theta} (b - b_0) [V_1 \cos \phi + V_2 \cos 2\phi + V_3 \cos 3\phi] \\
&+ \sum_{b'} \sum_\phi F_{b\theta} (b' - b'_0) [V_1 \cos \phi + V_2 \cos 2\phi + V_3 \cos 3\phi] \\
&\sum_\theta \sum_\phi F_{b\theta} (\theta - \theta_0) [V_1 \cos \phi + V_2 \cos 2\phi + V_3 \cos 3\phi] \\
&+ \sum_\phi \sum_\theta \sum_{\theta'} K_{\phi\theta\theta'} \cos \phi (\theta - \theta_0)(\theta' - \theta'_0) + \sum_{i>j} \frac{q_i q_j}{\epsilon r_{ij}} + \sum_{i>j} \left[\frac{A_{ij}}{r_{ij}^9} - \frac{B_{ij}}{r_{ij}^6} \right] \tag{2}
\end{aligned}$$

where K , H , F , A and B are constants, b is the bond distance, θ is bond angle, ϕ is related to torsion, and V is coefficient of cosine Fourier expansion. Terms from five to eleven in the equation (2) are crossterms which are bond or angle

distortions caused by nearby atoms. These off-diagonal cross-coupling terms make COMPASS a very unique and attractive forcefield, because other force fields have very limited capability in considering cross-coupling effects. However, it is also noted that COMPASS takes longest calculation time, and it may not cover some elements (materials).

UFF, which was developed in 1992 by Rappé, et al.[17], however, covers the full periodic table. UFF is usually employed for organometallic systems or systems other forcefields do not have the proper parameters [25]. The potential energy of UFF is expressed as:

$$\begin{aligned}
 E_{total}^{UFF} &= E_R + E_\theta + E_\phi + E_\omega + E_{vdw} + E_{el} \\
 &= \frac{1}{2} K_{IJ} (r - r_{IJ})^2 + K_{LJK} \sum_{n=0}^m C_n \cos n\theta + K_{LJKL} \sum_{n=0}^m C_n \cos n\phi_{LJKL} \\
 &\quad + K_{LJKL} (C_0 + C_1 \cos \omega_{LJKL} + C_2 \cos 2\omega_{LJKL}) \\
 &\quad + D_{IJ} \left\{ -2 \left[\frac{x_{IJ}}{x} \right]^6 + \left[\frac{x_{IJ}}{x} \right]^{12} \right\} + 332.0637 \left(\frac{Q_i Q_j}{\epsilon R_{ij}} \right)
 \end{aligned} \tag{3}$$

where K_{ij} , K_{ijkl} , and K_{ijkl} are force constants, θ is the periodic angle in Fourier expansion, C_n is the expansion coefficient defined by the natural bond angle θ_0 , r represents bond length, r_0 represents the natural bond length, and ω_{LJKL} is the angle between the il axis and ijk plane. D_{ij} is the well depth while x_{IJ} is the van der Waals bond length. The UFF possesses a parameter generator which combines atomic parameters to reproduce forcefield parameters for any combination of forcefield types.

One may notice that the angle bending, torsions and inversions are all described by cosine-Fourier expansion terms. The expression does not contain crossterms as they appeared in COMPASS forcefield potential energy. Its functional form is very simple so that the computation time can be minimal.

DREIDING was introduced by Mayo, et al. [18] in 1990. It is another generic and simple forcefield, which is useful in the prediction of structures and dynamics of organic, biological and main-group inorganic molecules. The potential energy of DREIDING forcefield is expressed as:

$$\begin{aligned}
 E_{total}^{Dreiding} &= E_{val} + E_{nb} \\
 &= (E_B + E_A + E_T + E_I) + (E_{vdw} + E_Q + E_{hb}) \\
 &= \frac{1}{2} k_e (R - R_e)^2 + \frac{1}{2} C_{LJK} [\cos \theta_{LJK} - \cos \theta_J^0]^2 + \frac{1}{2} V_{JK} \left\{ 1 - \cos [n_{JK} (\varphi - \varphi_{JK}^0)] \right\} \\
 &\quad + \frac{1}{2} K_{inv} (\psi - \psi_0)^2 + D_0 [\rho^{-12} - 2\rho^{-6}] + 332.0637 \left(\frac{Q_i Q_j}{\epsilon R_{ij}} \right) \\
 &\quad + D_{hb} \left[5 \left(\frac{R_{hb}}{R_{DA}} \right)^{12} - 6 \left(\frac{R_{hb}}{R_{DA}} \right)^{10} \right] \cos(\theta_{DHA})
 \end{aligned} \tag{4}$$

where E_B , E_A , E_T , E_I and E_{hb} represent the energy of bond stretch, bond angle bend, dihedral angle torsion, inversion and hydrogen bond. K , C , V are constants, D_0 is the van der Waals well depth, $\rho = R/R_0$ is the scaled distance, R_0 is the van der Waals bond length, Q is charge, D_{hb} , R_{hb} , R_{DA} are all hydrogen parameters. The DREIDING does not generate parameters in the way that UFF does automatically [25]. The DREIDING is simply to use general force constants and geometry parameters based on so-called hybridization considerations rather than

on individual force constants and geometric parameters that depend on the particular combination of atoms (eg. proteins, organics) involved in the bond, angle, or torsion terms.

The three forcefields have similar terms for stretching, van der Waals (COMPASS uses 6-9 type while Universal and DREIDING use 9-12 type Lennard-Jones type expression) and electrostatic interactions. Although Universal covers the full periodic table, its energy expression is purely diagonal and harmonic. The COMPASS force field has more complicated coupling cross terms than the other two forcefields. The COMPASS does not cover some materials, but it covers most common organic molecules, polymers, small gas molecules, inorganic materials including metals (Al, Fe, Mg etc), metal halides (Ca⁺⁺, Fe⁻ etc), Silica/Aluminosilicates (SiO₂, AlO₂) and metal oxides (CaO, Al₂O₃, SiO₂ etc.) [26].

Mechanical Properties Calculation

After a molecular dynamics simulation has been performed, the resulting deformed molecular structure was analyzed to determine elastic constants. Elastic constants of the final atomic configuration are computed using the static approach suggested by Theodorou and Suter [27]. The elastic stiffness coefficients, which relate the components of stress and strains, are defined as:

$$C_{lmnk} = \left. \frac{\partial \sigma_{lm}}{\partial \varepsilon_{nk}} \right|_{T, \varepsilon_{nk}} = \frac{1}{V_o} \left. \frac{\partial^2 A}{\partial \varepsilon_{lm} \partial \varepsilon_{nk}} \right|_{T, \varepsilon_{lm}, \varepsilon_{nk}} \quad (5)$$

where, A denotes the Helmholtz free energy, ε is the strain component, σ is the stress component and V_o is the volume of the simulation cell in the undeformed configuration. The energy-minimized structure is subjected to various deformations, and the elastic stiffness coefficients can be obtained by estimating the second derivations of the deformation energy with respect to strains, or the first derivative of the stress with respect to strain [25]:

$$\frac{d^2 E}{d\varepsilon_i d\varepsilon_j} = \frac{d\sigma_i}{d\varepsilon_j} \quad (6)$$

where, E is the potential energy of the system.

We can calculate the corresponding isotropic polycrystalline elastic moduli based on the corresponding single-crystal elastic constants (MD results of single crystals: elastic stiffness constants C_{ij} and elastic compliance constants S_{ij}) [28-29]. The Voigt-Reuss-Hill (VRH) approximation is a useful scheme which can be used to perform this task. According to Hill [30], VRH approximation can simply be expressed as:

$$K_{VRH} = (K_V + K_R) / 2 \quad (7)$$

and

$$G_{VRH} = (G_V + G_R) / 2 \quad (8)$$

where V and R refer to the Voigt and the Reuss averages. They can be derived from Elastic stiffness constants C_{ij} and Elastic compliance constants S_{ij} by the following Eqs (9)-(12) shown below.

Voigt Average:

$$9K_V = (C_{11} + C_{22} + C_{33}) + 2(C_{12} + C_{23} + C_{31}) \quad (9)$$

$$15G_V = (C_{11} + C_{22} + C_{33}) - (C_{12} + C_{23} + C_{31}) + 3(C_{44} + C_{55} + C_{66}) \quad (10)$$

Reuss Average:

$$1/K_R = (S_{11} + S_{22} + S_{33}) + 2(S_{12} + S_{23} + S_{31}) \quad (11)$$

$$15/G_R = 4(S_{11} + S_{22} + S_{33}) - 2(S_{12} + S_{23} + S_{31}) + 3(S_{44} + S_{55} + S_{66}) \quad (12)$$

Where G and K are shear and bulk moduli, respectively.

4. RESULTS AND DISCUSSIONS

Molecular Dynamics with three common forcefields, two MD tools and the different sizes of supercell were used to simulate the single crystals of cement constituents C_3S , C_2S and C_3A . Typical stiffness and compliance matrices obtained for simulation of $1a \times 1b \times 1c$ C_3S supercell using COMPASS forcefield with Forcite MD tool are shown below.

- Elastic Stiffness Constants C_{ij} (GPa) of C_3S :

$$C_{ij} = \begin{bmatrix} 132.0832 & 71.3912 & 49.3632 & 21.6456 & -6.4990 & 1.5686 \\ 71.3912 & 211.6644 & 124.8335 & -4.1212 & 0.5856 & -0.5979 \\ 49.3632 & 124.8335 & 234.2412 & 2.4543 & 5.7832 & -1.9870 \\ 21.6456 & -4.1212 & 2.4543 & 57.4192 & 0.1954 & 0.0241 \\ -6.4990 & 0.5856 & 5.7832 & 0.1954 & 56.9348 & -0.6179 \\ 1.5686 & -0.5979 & -1.9870 & 0.0241 & -0.6179 & 50.6488 \end{bmatrix} \quad (13)$$

- Elastic Compliance Constants S_{ij} (1/TPa) of C_3S

$$S_{ij} = \begin{bmatrix} 10.2395 & -3.3109 & -0.3845 & -4.0854 & 1.2521 & -0.3541 \\ -3.3109 & 7.9904 & -3.5783 & 1.9749 & -0.1028 & 0.0543 \\ -0.3845 & -3.5783 & 6.2787 & -0.3782 & -0.6413 & 0.2083 \\ -4.0854 & 1.9749 & -0.3782 & 19.1155 & -0.5125 & 0.1197 \\ 1.2521 & -0.1028 & -0.6413 & -0.5125 & 17.7765 & 0.1519 \\ -0.3541 & 0.0543 & 0.2083 & 0.1197 & 0.1519 & 19.7654 \end{bmatrix} \quad (14)$$

We substituted equations (13) and (14) into equations (7)-(12) and get the isotropic elastic properties of C_3S shown in Table 2 Column 3. Table 2 provides a summary of the MD computation results of C_3S . The results of C_3S are obtained by the following combinations: (1) Discover with COMPASS forcefield (D-C); (2) Forcite together with COMPASS forcefield (F-C); and (3) Forcite with UFF (F-U). Since the F-U combination did not produce reasonable results compared to those of F-C and D-C combinations, we simply discard it for $2a \times 2b \times 2c$ supercell computation. Compared with the nano-indentation test results, we concluded that the best choice for the simulation of C_3S is a F-C combination though D-C also yields good results.

Based on the results of C_3S , we mainly used combinations of D-C and F-C in the simulation of C_2S . The computation results for C_2S are given in Table 3, which again indicates that FC combination matches the experimental values with good accuracy. We also observed that a F-U combination underestimates the modulus values for both C_3S and C_2S . MD simulation results for C_3A are shown in Table 4. The F-C combination did not work for C_3A , so no corresponding results are given in the table.

MD Modules (Tools)

To further explore the different computation results between two different molecular mechanics modules, Forcite and Discover, one needs to take into account the following facts:

Forcite [31] is an advanced classical molecular mechanics tool, which calculates single point energies and performs geometry optimization (i.e. energy minimization) of molecules and periodic systems. For periodic systems, Forcite allows the optimization of the cell parameters simultaneously with the molecular coordinates. During a geometry optimization of a crystal structure, Forcite preserves the symmetry defined by the space group; the crystal structure is optimized either with respect to all structural degrees of freedom or by applying rigid body constraints where the relative distances between a group of atoms are fixed [25]. On the other hand, Discover provides the underlying calculations for products such as an Amorphous Cell. It also supports varied simulation strategies. Periodic boundary conditions allow the simulation of solid-state systems, whether crystalline or amorphous, or of solvated systems [25].

Therefore, it seems that Discover is able to handle both crystalline and amorphous structure, while Forcite is able to handle crystalline structures only. The Forcite looks somewhat inferior molecular mechanics module; however, it works within the known crystal structures and the structural degrees of freedom (such as known atomic distances). As a result, the Forcite may provide more accurate computational results as far as the crystalline structures are known. Discover may handle crystalline structures, but it does not utilize predetermined informations such as atomic distances to leverage the computation results; therefore, its

calculation results may not be as accurate as the Forcite module. At the same time, its calculation results may be as accurate as the Forcite module when the reasonable equilibrium condition is computed.

C_3S , C_2S and C_3A have well-defined crystal structures. Thus, it is natural that the Forcite calculation module produced more realistic results. The effects of the forcefield are also demonstrated as follows:

The COMPASS forcefield considers more coupling effects while UFF considers only a limited number of coupling effects. Therefore, it is reasonable that the COMPASS forcefield produced more realistic results. More in depth discussions of the forcefield may be found in [32].

Table 4 shows that the Forcite–DREIDING forcefield combination (F-D) produces more reasonable results than the Forcite-Universal combination (F-U).

5. CONCLUSIONS AND DISCUSSIONS

Molecular Dynamics study on the mechanical properties of major cement constituents revealed that:

The elastic moduli of C_3S , C_2S and C_3A are 137 GPa, 121 GPa and 144 GPa. The corresponding Poisson's ratios are 0.29, 0.19 and 0.22.

(1) The Forcite and COMPASS forcefield combination is appropriate for the simulation of C_3S , C_2S . The Forcite with DREIDING forcefield gives reasonable properties of C_3A but the Forcite and UNIVERSAL combination is not good for all of the simulations.

(2) Supercell size effect is not major compared with our previous work on the simulation of quartz-alpha [29].

Molecular Dynamics is a very useful tool in the computation of mechanical properties of cementitious materials as shown in this study. However, the computation time of MD simulation is tremendous for systems with a large number of atoms. A real ‘universal’ forcefield for the simulation of cementitious materials does not exist, which means the simulation is dependent on forcefields and the MD tools. Our previous work [29] on MD simulation of quartz-alpha indicates Discover with COMPASS is the best combination. Therefore, careful choosing of forcefield in MD simulation should be considered first and foremost.

The effect of two different molecular dynamics modulus used in the simulation is also briefly given. Forcite gives reasonable results for cement constituent materials though Discover is more widely used in MD simulation.

ACKNOWLEDGEMENTS

This work was partially supported by the funding received under a subcontract from the Department of Homeland Security-sponsored Southeast Region Research Initiative (SERRI) at the Department of Energy's Oak Ridge National Laboratory, USA.

REFERENCES:

- [1] Concrete. In Wikipedia, The Free Encyclopedia. Retrieved September 3, 2008, from <http://en.wikipedia.org/w/index.php?title=Concrete&oldid=235916630>
- [2] D.P. Bentz, C.J. Haecker, X.P. Feng, P.E. Stutzman, Process Technology of Cement Manufacturing, *Proceedings of the 5th International VDZ Congress*, September 23-27, Düsseldorf, Germany, 2003, pp 53-63.
- [3] American Society for Testing and Materials. ASTM Annual Book of Standards, Cement; Lime; Gypsum, Vol.04.01, PA: West Conshohocken 1999.
- [4] D. Brehm, Nanoengineered concrete could cut carbon dioxide emissions. Retrieved March 12, 2008, from <http://web.mit.edu/newsoffice/2007/concrete.html>
- [5] MIT's Department of Civil and Environmental Engineering, On Balance: Nanoengineered concrete could cut world CO₂. [Brochure]. Cambridge, MA: Denise Brehm (ed), 2007.
- [6] K. Velez., S. Maximilien, D. Damidot, G. Fantozzi, F. Sorrentino, Determination by nanoindentation of elastic modulus and hardness of pure constituents of Portland cement clinker, *Cement and Concrete Research* 31(4) (2001) 555-561.
- [7] A. Boumiz, D. Sorrentino, C. Vernet, F.C. Tenoudji, Modelling the development of the elastic moduli as a function of the degree of hydration of cement pastes and mortars, in Proceedings 13 of the 2nd RILEM Workshop

on Hydration and Setting: Why does cement set? An interdisciplinary approach, edited by A. Nonat (RILEM Dijon, France, 1997); A. Boumiz, Thèse de Doctorat d'Acoustique Physique, Université Paris 7 (1995) (Denis Diderot).

- [8] J.L.Granju, Modélisation des pates de ciments durcies: Caractérisation de l'état d'hydratation, lois d'évolution de la résistance en compression et du module de déformation longitudinale, PhD thesis, Université Paul Sabatier de Toulouse, France, 1987.
- [9] P.E. Garcia-Casillas, C.A Martinez, H. Montes, Camacho; Garcia-Luna. A.Prediction of portland cement strength using statistical methods, *Materials and Manufacturing Processes* 22(3) (2007) 333-336.
- [10] A.Baykasoglu, Dereli, Turkey, Tanis, Serkan. Prediction of cement strength using soft computing techniques, *Cement and Concrete Research* 34(11) (2004) 2083-2090.
- [11] A. Al-Ostaz, G. Pal., P. R. Mantena, A. Cheng, Molecular dynamics simulation of SWCNT-polymer nanocomposite and its constituents, *Journal of Materials Science* 43(1) (2008) 164-173.
- [12] P.R Mantena, A. Al-Ostaz, A. Cheng, Dynamic Response and Simulations of nanoparticle-Enhanced Composites, *Composite science and technology*, Submitted.
- [13] V.V. Ivanovskaya, N. Ranjan, T. Heine, G. Merino, G. Seifert, Molecular dynamics study of the mechanical and electronic properties of carbon nanotubes, *Small* 1(4) (2005) 399-402.

- [14] R.Zhu, E. Pan, A.K. Roy, Molecular dynamics study of the stress-strain behavior of carbon-nanotube reinforced Epon 862 composites Source, Materials Science and Engineering, 447(1-2) (2007) 51-57.
- [15] H.F.W. Taylor, Cement Chemistry, 2nd Edition, Thomas Telford, London, England, 1997.
- [16] H. Sun, P. Ren, J.R. Fried, The COMPASS Force Field: parameterization and validation for phosphazenes, Comput. Theor. Polymer Sci. 8 (1998) 229-246.
- [17] A.K. Rappe, C.J. Casewit, K.S. Colwell, W.A. Goddard III, W.M. Skiff, UFF, a full periodic table force field for molecular mechanics and molecular dynamics simulations, J. Am.Chem. Soc. 114(25) (1992) 10024-10035.
- [18] S.L. Mayo, B.D. Olafson, and W.A. Goddard III, DREIDING: a generic force field for molecular simulations, J. Phys. Chem. 94 (1990) 8897-8909.
- [19] C.R. Song, H. Cho, Y-H. Jung, A. H-D. Cheng, and A. Al-Ostaz, Bridging Molecular, Particulate and Continuum Mechanics for Geomechanics Application, GeoDenver 2007 (2007) CD-Rom
- [20] N. I. Golovastikov, R.G.Matveeva, N.V. Belov, Crystal structure of the tricalcium silicate $3\text{CaO} \cdot \text{SiO}_2 = \text{C}_3\text{S}$, Sov. Phys. Crystallogr. 20 (4) (1975) 441.
- [21] C.M. Mideley, The crystal structure of β dicalcium silicate, Acta Cryst. **5**, (1952) 307-312.
- [22] P. Mondal, J.W. Jeffery, The crystal structure of tricalcium aluminate, $\text{Ca}_3\text{Al}_2\text{O}_6$, Acta Cryst. B31 (1975) 689-697.

- [23] R.T.Cygan, J.D. Hubicki (eds). Molecular modeling theory: applications in the geosciences, Reviews in mineralogy and geochemistry 42 (2001) Geochemical society, Washington DC.
- [24] Materials Studio 4.2, Accelrys: San Diego, CA, 2008.
- [25] Accelrys Inc., Materials Studio 4.2 Manual, San Diego.
- [26] The Scripps research institute, COMPASS, Ewreiwews March 18, 2008, from The Scripps research institute website: <http://www.scripps.edu/rc/softwaredocs/msi/cerius45/compass/COMPASSTC.doc.html>.
- [27] D.N. Theodorou, U. W. Suter, Atomistic Modeling of Mechanical Properties of Polymeric Glasses, Macromolecules 19 (1986) 139 – 154.
- [28] R.S. Carmichael, Handbook of physical properties of rocks, vol 2, CRC Press, Boca Raton, 1982.
- [29] D.H. Chung, W.R. Buessem, The Voigt-Reuss-Hill(VRH) approximation and the elastic moduli of polycrystalline ZnO, TiO₂, and α -Al₂O₃, Journal of applied physics 39(6) (1968) 2777-2782.
- [30] R. Hill, The elastic behavior of a crystalline aggregate, Proc. Phys. Soc. 65 (1952) 349-354.
- [31] Accelrys Inc., Forcite data sheet, Retrieved September 3, 2008, from http://accelrys.com/products/datasheets/ms_forcite.pdf
- [32] C.R. Song, C.R., W. Wu, A. Al-Ostaz, Effects of Force Field in Molecular Mechanics Simulation of Geo-Materials, Submitted to Mechanics Research Communications. Submitted for publication.

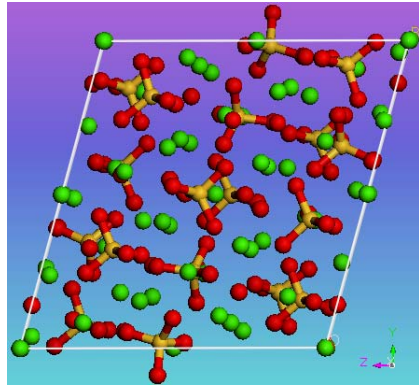


Figure 1. Unit Cell Crystal Structure of C_3S : projection view along the $[100]$ direction. The green ball is Calcium (Ca), the dark orange ball is silicate (Si), the pink tetrahedral is aluminum (Al), and the red ball is oxygen (O).

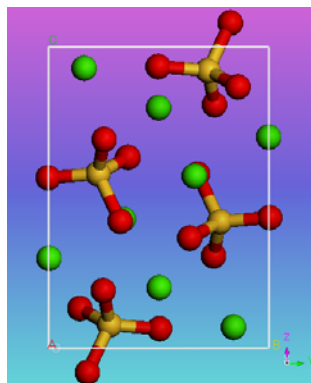
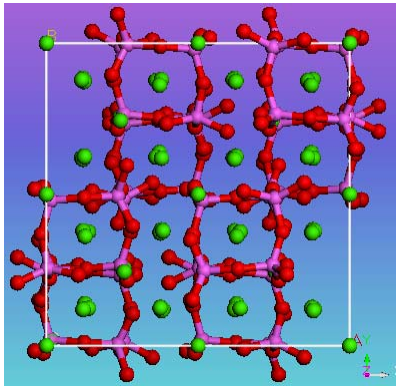


Figure 2. Unit Cell Crystal Structure of C₂S: projection view along the [100] direction.



(c)

Figure 3. Unit Cell Crystal Structure of C₃A: projection view along the [001] direction.

Table 1. Cell Parameters of C₃S, C₂S and C₃A Crystals

Crystal	C ₃ S	C ₂ S	C ₃ A
Space	P-1	P21/n	Pa3
a [Å]	11.67	5.48	15.263
b [Å]	14.24	6.76	15.263
c [Å]	13.72	9.28	15.263
α[o]	105.5	90	90
β[o]	94.33	94.33	90
γ[o]	90	90	90
Reference	[23]	[24]	[25]

Table 2. MD Simulation Results of C₃S

Supercell	1a×1b×1c		2a×2b×2c			Ref
Properties						Values
MD Tools & Forcefield	D-C	F-C	F-U	D-C	F-C	
E	168	137	45.4	139	148	135 ^[2] 117 ^[3] 60~300 ^[4]
ν	0.34	0.29	0.26	0.36	0.35	0.31 ^[3]
κ	180	110	31.8	171	168	-
G	63	53	18	51	54.8	-

E: Elastic Modulus (GPa) ν : Poisson's Ratio κ : Bulk Modulus G:

Shear Modulus

D-C: Discover with COMPASS, F-C: Forcite with COMPASS, F-U: Forcite with
Universal

Table 3. Molecular Simulation Results of C₂S

Supercell								Ref
Properties	1a×1b×1c		2a×2b×2c		3a×3b×3c		Value	
MD Tools & Forcefield	D-C	F-C	F-U	D-C	F-C	D-C	F-C	
E	285	122	57.7	265	121	262	121	130 ^[2]
ν	0.23	0.19	0.35	0.22	0.19	0.22	0.19	0.31 ^[3]
κ	177	65	63.2	161	64	161	64	-
G	116	51	21.4	108	51	108	51	-

Table 4. Molecular Simulation Results of C₃A

Supercell Properties					Ref Value
	1a×1b×1c		2a×2b×2c		
MD Tools & Forcefield	F-U	F-D	F-U	F-D	
E	70	141	66.3	-	145 ^[2]
v	0.31	0.22	0.32	-	0.31 ^[3]
κ	63	84	59.8	-	-
G	26.6	58	25.2	-	-

F-D: Forcite with DREIDING